Optimization of Two-Compartment-Exchange-Model Analysis for Dynamic Contrast-Enhanced MRI Incorporating Bolus Arrival Time

Guy Nadav, MSc,[1,2] Gilad Liberman, PhD,[1,3] Moran Artzi, PhD,[1] Nahum Kiryati, PhD,[2] and Dafna Ben Bashat, PhD[1,4,5]*

Purpose: To optimize the analysis of dynamic contrast-enhanced magnetic resonance imaging (DCE-MRI) under the two-compartment-exchange-model (2CXM) and to incorporate voxelwise bolus-arrival-time (BAT).
Materials and Methods: The accuracy of the pharmacokinetic (PK) parameters, extracted from 3T DCE-MRI using 2CXM, was tested under several conditions: eight algorithms for data estimation; correction for BAT; using model selection; different temporal resolution and scan duration. Comparisons were performed on simulated data. The best algorithm was applied to seven patients with brain tumors or following stroke. The extracted perfusion parameters were compared to those of dynamic susceptibility contrast MRI (DSC-MRI).
Results: ACoPeD (AIF-corrected-perfusion-DCE-MRI), an analysis using a 2nd derivative regularized-spline and incorporating BAT, achieved the most accurate estimation in simulated data, mean-relative-error: F_p, F, v_p, v_e: 24.8%, 41.7%, 26.4%, 27.2% vs. 76.5%, 190.8%, 78.8%, 82.39% of the direct four parameters estimation (one-sided two-sample t-test, $P < 0.001$). Correction for BAT increased the estimation accuracy of the PK parameters by more than 30% and provided a supertemporal resolution estimation of the BAT (higher than the acquired resolution, mean-absolute-error 0.2 sec). High temporal resolution (~2 sec) is required to avoid biased estimation of PK parameters, and long scan duration (~20 min) is important for reliable permeability but not for perfusion estimations, mean-error-reduction: E: ~12%, v_e: ~6%. Using ACoPeD, PK values from normal-appearing white matter, gray matter, and lesion were extracted from patients. Preliminary results showed significant voxelwise correlations to DSC-MRI, between flow values in a patient following stroke ($r = 0.49$, $P < 0.001$), and blood volume in a patient with a brain tumor ($r = 0.62$, $P < 0.001$).
Conclusion: This study proposes an optimized analysis method, ACoPeD, for tissue perfusion and permeability estimation using DCE-MRI, to be used in clinical settings.

J. MAGN. RESON. IMAGING 2016;00:000–000.

Quantification of perfusion and vessel permeability in the human body and brain is of some clinical importance. Within the brain, dynamic contrast-enhanced magnetic resonance imaging (DCE-MRI) is commonly used to estimate permeability-related pharmacokinetic (PK) parameters. A widely used model for DCE-MRI analysis is the three-parameter Extended Toft's Model (ETM),[1] which includes the volume transfer constant (K^{trans}), plasma volume (v_p), and extravascular extracellular space (v_e). Most models used in DCE-MRI analysis neglect perfusion-related parameters such as the cerebral blood flow (CBF). For perfusion extraction, the four-parameter two-compartment exchange model (2CXM) is commonly used,[2–4] and has shown promising results for estimating CBF, cerebral blood volume (CBV), and permeability from DCE-MRI,[3,4] although alternative models are available.[1] However, the estimation process, techniques, and corrections for inaccuracies in the 2CXM model vary among research groups.[2–8]

View this article online at wileyonlinelibrary.com. DOI: 10.1002/jmri.25362

Received Oct 17, 2015, Accepted for publication Jun 10, 2016.

*Address reprint requests to: D.B.B., Wohl Institute for Advanced Imaging, Tel Aviv Sourasky Medical Center, 6 Weizman St. Tel-Aviv 64239 Israel. E-mail: dafnab@tlvmc.gov.il

From the [1]Functional Brain Center, Wohl Institute for Advanced Imaging, Tel Aviv Sourasky Medical Center, Tel Aviv, Israel; [2]School of Electrical Engineering, Tel Aviv University, Tel Aviv, Israel; [3]Department of Chemical Physics, Weizmann Institute, Rehovot, Israel; [4]Sackler Faculty of Medicine, Tel Aviv University, Tel Aviv, Israel; and [5]Sagol School of Neuroscience, Tel Aviv University, Tel Aviv, Israel.

Additional Supporting Information may be found in the online version of this article.

Methods for DCE-MRI analysis varied between studies. In a thorough discussion, Sourbron et al[4] present different monoexponential regimes for exchange models, and suggested estimating the parameters of the full four-parameter model using a nonlinear curve fitting on the concentration–time curve (CTC) with a variation of the Levenberg–Marquardt algorithm.[9] The analysis was done using the assumption that the signal is proportional to the relaxation rate ($1/T_1$), which is only valid for low-contrast agent concentrations. Larson et al[2] proposed a computationally exhaustive generalized singular value decomposition approach for the deconvolution problem.

Bolus arrival time (BAT) has been shown to have an impact on the estimated parameters when the analyzed area is distant from the location where the arterial-input-function (AIF) was measured.[10–12] Previous works on dynamic susceptibility contrast MRI (DSC-MRI)[13–15] describe the problem of estimating perfusion under bolus delay (referred to here as BAT) and dispersion. A circular deconvolution method was previously proposed,[15] which constructs a block-circulant deconvolution matrix that is time-invariant and reduces the sensitivity of the estimated perfusion parameters to BAT. However, BAT estimation in DCE-MRI analysis has received limited attention, probably due to the low temporal resolution (~6 sec) commonly used, which is much longer than the intertissue difference.[13] Accounting for BAT was recently shown to improve the accuracy of the estimated ETM parameters in DCE-MRI.[16] Kershaw and Buckley[11] suggested estimation of BAT in DCE-MRI using the adiabatic approximation to the tissue homogeneity (AATH) model, based on the linear-quadratic model (LQ-model) originally proposed by Cheong et al.[17] This analysis assumes that contrast agent exchange only takes place at the venous end of the capillary bed, and although it often forms a good approximation, this assumption cannot be justified physiologically, especially in the brain.[1] In this prior study we incorporated BAT into the 2CXM, which is the most commonly used four-parameter model applied to DCE-MRI in the brain.[1]

Using the correct model is very important for accurate estimation and interpretation of the PK maps. Ewing et al[18] thoroughly demonstrated the use of model selection in DCE-MRI, using a nested three-parameter model with F-test criterion on clinical data. Buckley and Sourbron[7] addressed model selection for four-parameter models and suggested using the Akaike information criterion, while Ingrisch et al used model selection with Akaike information criterion and Akaike weights to estimate perfusion and permeability parameters in patients with multiple sclerosis.[8]

The aim of this study was to optimize the analysis method for DCE-MRI under 2CXM while incorporating voxelwise BAT. The starting point of the method proposed in this study is the work of Larson et al[2,3] and advancements in the analysis model are based on Sourbron et al.[1,4,7] Several advances are proposed in this study: improvement in accurate approximation to the AIF convolution matrix using a piecewise linear discretization; a simple transformation of the generalized singular value decomposition to a standard ridge regression formulation; selection of the regularization term; and using the Akaike information criterion with correction for finite sample sizes for model selection.

Theory

ACoPeD (AIF-Corrected Perfusion DCE-MRI): The Suggested Algorithm for 2CXM Parameter Estimation

The model chosen in this method is an updated version of the 2CXM described by Larsson et al[3] and based on the model standardization presented by Sourbron and Buckly,[1] consisting of v_p, v_e, plasma flow (F_p), and permeability–surface area product (PS). To estimate the 2CXM's parameters we followed the model-free deconvolution as described by Larsson et al[3] which treats the CTC as a convolution of the AIF and an impulse response function (IRF).

Figure 1 shows the general scheme of the proposed method. The CTC was deconvolved with the AIF to estimate the IRF. The deconvolution was performed using the minimization of a cost function given in a matrix form. The full derivation of the minimization problem for the model-free IRF estimation is given in Supporting Appendix 1. The final minimization problem is described in Eq. 1:

$$\|D'_{V'} - C\|^2 + \lambda^2 \|_{V'} - {}_{V'_o}\|^2 \qquad (1)$$

Where $|D' \triangleq ABL^{-1}$, ${}_{V'} \triangleq L_V$, ${}_{V'_0} \triangleq L_{V0}$.

A is the AIF convolution matrix, B is the basis functions matrix, V is the basis coefficients vector, V_o is the initial estimation for the basis coefficients vector and L is a matrix operator (eg, derivative estimation). After solving for V', one can extract the IRF by $IRF = BL^{-1}V'$ (see Supporting Appendix 2), which shows how this regularized minimization problem can be transformed into a standard form. This enabled the use of a simple ridge regression instead of the computationally expensive generalized singular value decomposition.[3] To enforce prior assumptions (eg, smoothness) on the IRF, it was modeled as a linear combination of basis functions, ie:

$$IRF = Basis\_Matrix \cdot Coefficients\_Vector$$

using a cubic-spline basis with a reduced number of eigenvectors to reduce the number of free parameters in the minimization problem, as previously suggested[2,3] (with N/5, where N is the number of data samples).

Piecewise linear discretization of the AIF,[13] instead of the piecewise-constant discretization,[3] was used In ACoPeD, to enhance accuracy in the discretization of the convolution integral with no computational cost. This is shown in Supporting Appendix 1, Eq. [A1.4].

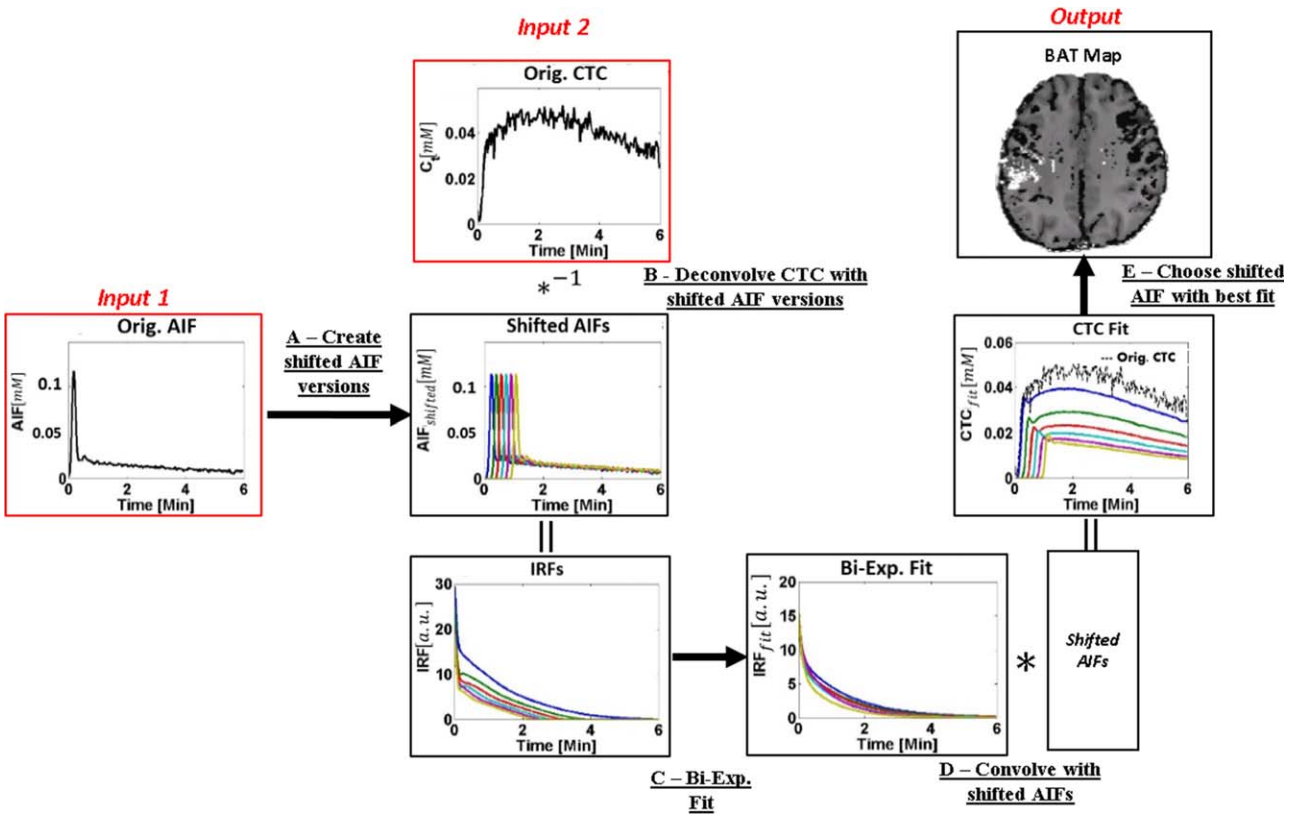

FIGURE 1: ACoPeD (AIF corrected perfusion DCE-MRI) flow chart. Given a concentration–time curve (CTC) and an arterial-input-function (AIF), a set of shifted versions of the AIF is created (A). The CTC is deconvolved with every shifted version (B) and the resulting impulse response functions (IRFs) are then fitted to the 2CXM biexponential model (C). The fitted IRFs are then convolved back with shifted AIFs (D) and the shifted AIF corresponding to the best fit (marked in blue) is chosen (E).

After estimating the IRF, F_p was set to be the maximal value of the IRF. A nonlinear biexponent fit to the IRF was then carried out to estimate the other PK parameters, while keeping F_p fixed.

BAT Correction Using ACoPeD

To estimate the voxelwise BAT and to improve the accuracy of the PK parameters estimation, the following procedure was used (see Fig. 1):

A: The AIF was upsampled, (ie, more data points were estimated) using piecewise cubic interpolation, and then shifted in superresolution time steps (eg, 0.1 second shift when the data are at 2-second resolution).

B: The CTC was deconvolved with varying predetermined shifted versions of the measured AIF to get possible IRFs.

C: F_p was fixed to be the maximal IRF value. The IRFs were then fitted to a biexponent model, which reflects the four-parameter 2CXM.

D: Each of the fitted IRFs was convolved with the corresponding shifted AIF to produce CTC estimation.

E: The shift that minimized the root mean square (RMS) error between the estimated CTC and the measured one was used as the BAT.

This method forced the IRF into a biexponential shape, while providing a good fit to the data. The computation time increases linearly with the number of AIF shifts, ie, is inverse to the desired temporal resolution of the BAT estimation, and to the BAT range.

Model Selection in ACoPeD

Model selection was done using the corrected Akaike information criterion, to compensate for finite sample size. In total, five models were calculated based on model boundary regimes, as discussed by Sourbron et al[1,4]: four-parameter 2CXM (F_p, E, v_p, v_e), three-parameter compartment-uptake model (F_p, E, v_p), two-parameter highly vascularized / no contrast agent exchange (F_p, v_p), one-parameter, highly perfused with no contrast agent exchange (v_p), and no contrast agent in the tissue (the null hypothesis). BAT was considered an additional parameter in the first four models, resulting in nine possible models.

Materials and Methods

Overview

To test the accuracy of the proposed ACoPeD method, we compared its results to six different deconvolution techniques and to an algorithm that was previously suggested[4] (a total of eight comparisons) without adding BAT to the simulations. To test the effect

TABLE 1. 2CXM Parameter Estimation: Analysis Techniques

	Mean relative error ± SEM [%]						
	Analysis technique						
	Spline	**Spline 1st**	**Spline 2nd**	**PCA**	**PCA 1st**	**PCA 2nd**	**Wiener**	**Direct 4-params**
F_P	28.90 ± 0.48	28.76 ± 0.48	24.82 ± 0.67	47.42 ± 0.64	40.92 ± 0.66	32.28 ± 0.65	39.74 ± 0.85	76.58 ± 10.99
E	189.78 ± 12.30	150.58 ± 11.11	41.72 ± 3.20	237.50 ± 12.61	226.11 ± 13.07	221.01 ± 13.47	163.2 ± 11.7	190.85 ± 34.48
V_P	35.88 ± 2.52	38.00 ± 2.38	26.41 ± 1.54	33.32 ± 1.50	33.62 ± 1.27	36.29 ± 1.95	44.11 ± 6.23	78.88 ± 13.74
V_e	49.73 ± 1.10	33.51 ± 1.13	27.29 ± 0.94	59.50 ± 1.25	56.62 ± 1.05	54.21 ± 1.07	49.49 ± 5.28	82.39 ± 15.23

Mean and standard error of the mean (SEM) [in %] of the 2CXM parameters, estimated using different analysis techniques.

of incorporating BAT on the accuracy of parameter estimation, BAT was added in simulation and ACoPeD's estimation accuracy was compared with three algorithms that were previously suggested to deal with BAT (a total of four algorithms). To investigate the contribution of using model selection, the parameters were estimated assuming a full five-parameter model and using model selection. ACoPeD was additionally tested for different temporal resolutions and scan durations in simulations. We then applied the optimized method to data from patients and compared flow and blood volume parameters extracted from DCE-MRI to those extracted from DSC-MRI. ACoPeD was coded in MatLab (MathWorks, Natick, MA), and a publicly available implementation of the method is offered.

Simulated Data

CTC GENERATION. An AIF was simulated using a population averaged AIF[19] and convolved through 1000 IRFs with varying parameter values, generated from uniform distributions over physiologically feasible ranges: F_p: 10–150 [mL/100mL/Min], extraction fraction (E): 0–0.5 [arbitrary units (a.u.)], v_p: 3–20 [mL/100mL], v_e: 3–20 [mL/100mL].[3] According to Larsson et al,[3] estimation is acceptable as long as permeability is not too large ($E < 0.5$), which is often the case with real data.[3] The IRFs were built using the 2CXM and the convolved results were set as the CTCs. These values were used as ground truth for validation. Gaussian noise was added to the AIF and the CTCs in order to obtain a realistic contrast-to-noise ratio (CNR) of 15.[3] CNR was defined as the mean concentration value divided by the CTC noise standard deviation. All simulated CTCs were 6 minutes long with 2 seconds temporal resolution, unless otherwise specified.

COMPARING DIFFERENT METHODS FOR PARAMETER ESTIMATION. A total of eight different methods for estimation of the PK parameters using 2CXM were tested and compared: seven methods with different deconvolution techniques and a direct four-parameter nonlinear fit using the Levenberg–Marquardt algorithm[4] (Table 1). Two methods were used to construct a linear combination of basis functions for the IRF: a cubic spline basis (as used in ACoPeD) and principal component analysis (PCA), which was built from the eigenvectors of typical values 2CXM IRFs, to minimize the reconstruction error.[20] PCA basis vectors were built by generating 100,000 2CXM IRFs with parameters uniformly distributed in the mentioned typical range, from which the first N/5 components were taken. The cubic-spline and PCA methods were tested with an additional 1st and 2nd derivative operator on the regularization term[4] to ensure smooth solutions. Higher derivatives were tested but did not improve accuracy (data not presented). Constraining for a smooth IRF was also performed using a Wiener filter[21] for the deconvolution step.

BAT CORRECTION AND PARAMETER ESTIMATION. Simulated data were created by adding varying time shifts to the AIF before convolving, from a uniform distribution in the range of 0–20 seconds with 0.1 seconds temporal resolution. This was done to simulate local BAT in the brain,[5] with respect to the measured AIF.[22] The accuracy of BAT estimation and the effect of incorporating BAT in the 2CXM model on the accuracy of the estimated PK

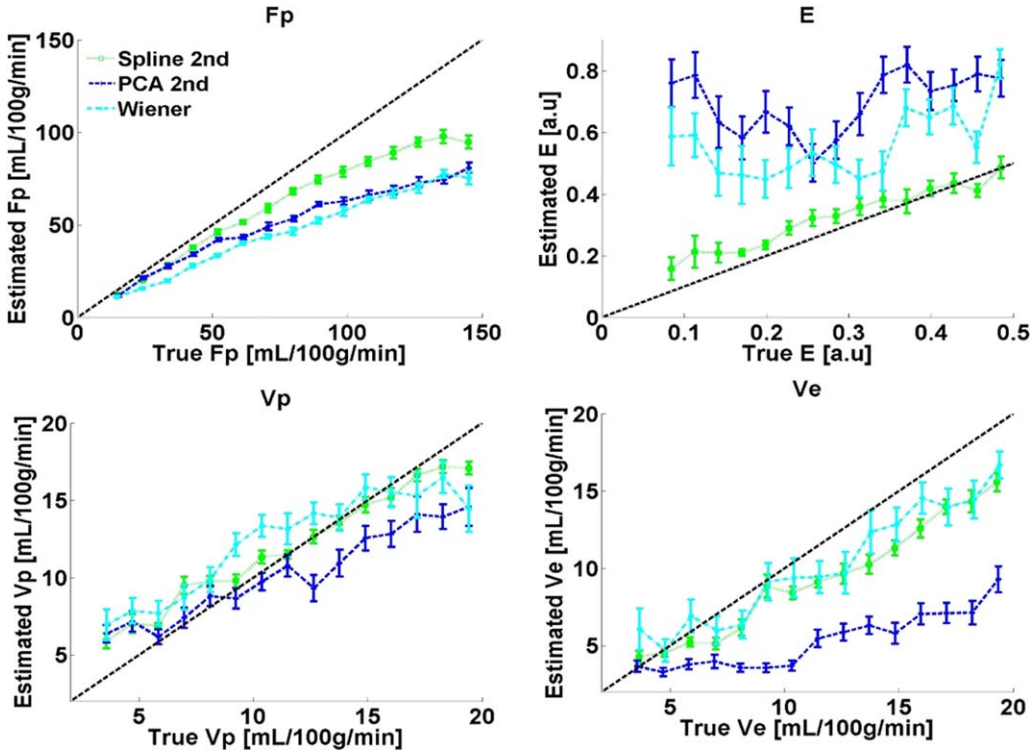

FIGURE 2: Estimation of PK parameters using different analysis techniques. Estimation values and SEM: green = Spline with 2nd derivative, blue = PCA with 2nd derivative, cyan = Wiener Filter, dashed black line = ground truth value.

parameters were tested using four methods: ACoPeD (Fig. 1); LQ-model[11]; circular deconvolution[15] with the IRF's maximum value time (MVT) as the BAT estimation; and ACoPeD with no BAT correction. The circular deconvolution is the common procedure for handling BAT in DSC-MRI[15] while the LQ-model showed good results when dealing with two-compartment models in DCE-MRI.[11]

CHOOSING THE CORRECT MODEL. Simulated AIFs were convolved with 1000 IRFs for eight models: 2CXM, compartment-uptake, highly vascularized, and highly perfused models (using the range for the parameters as described before), with and without BAT. All parameters were estimated twice, using ACoPeD (which assumes a full model and results in five parameters) and using the correct ground truth model.

EFFECT OF TEMPORAL RESOLUTION AND SCAN DURATION. Simulated AIF and CTCs were generated with a temporal resolution of 1 msec, and then subsampled to a temporal resolution of 2, 4, and 6 seconds before applying deconvolution estimation. The highest temporal resolution of 2 seconds was chosen based on a previous study suggesting that this temporal resolution is an acceptable resolution for perfusion estimation.[3]

For the effect of scan duration, PK parameters were estimated and compared to the ground truth values, using ACoPeD, for time durations of 6 and 20 minutes and using a temporal resolution of 2 seconds.

Data From Patients

Seven patients were included in this study, four patients with high grade brain tumors (biopsy proven glioblastoma, GB), and three patients following acute ischemic stroke, scanned 4–5 days following the event. Inclusion criteria for all subjects were normal glomerular filtration rate, and no contraindication to MRI scan. This study was approved by the hospital Review Board, and written informed consent was obtained from all patients.

MRI PROTOCOL. MRI scans were performed on a 3.0T MRI scanner (GE Signa Excite, Milwaukee, WI) using an eight-channel head coil, or Siemens system (Magnetom Prisma, Erlangen, Germany) using a 20-channel head coil. For the DCE-MRI data, eight slices, with 5 mm thickness and no gap, were acquired using multiphase 3D SPGR/FLASH T_1-weighted imaging, during injection of 0.2 cc/kg (single dose) gadolinium dotarem (gadoterate meglumine), using a power injector (Medrad, Pittsburgh, PA, Spectris Solaris EP), at a constant rate of 5 cc/sec, and with a delay of 30 seconds (field of view [FOV] / matrix = 250mm/256×256, TR/TE = 4.11/2.1 msec, flip angle [FA] = 20°, 180 repetitions in temporal resolution of 2 sec and a total scan time of 6 min). For the T_1 maps, variable FA spoiled SPGR (VFA-SPGR) data was acquired with nominal FAs = 5°, 10°, 15°, 20°, 30°. Slices were located at the center of the tumor / ischemic stroke area (as defined based on the anatomical images).

In two patients, one with GB and one following stroke, DSC-MRI data were additionally acquired ~15 minutes after DCE-MRI using a 2D gradient echo, echo planar imaging (GRE-EPI) sequence (19 slices with 5 mm thickness and no gap, with FOV/matrix = 220–240mm/128×128, TR/TE = 1300/30 msec, and 92 repetitions in temporal resolution of 1.3 sec and a total scan time of 2 min), during the injection of 0.4 cc/kg (double dose) of gadolinium dotarem at a constant rate of 5 cc/sec, after a delay of 15 seconds. A double dose was used as previously suggested when combined with DCE-MRI.[23]

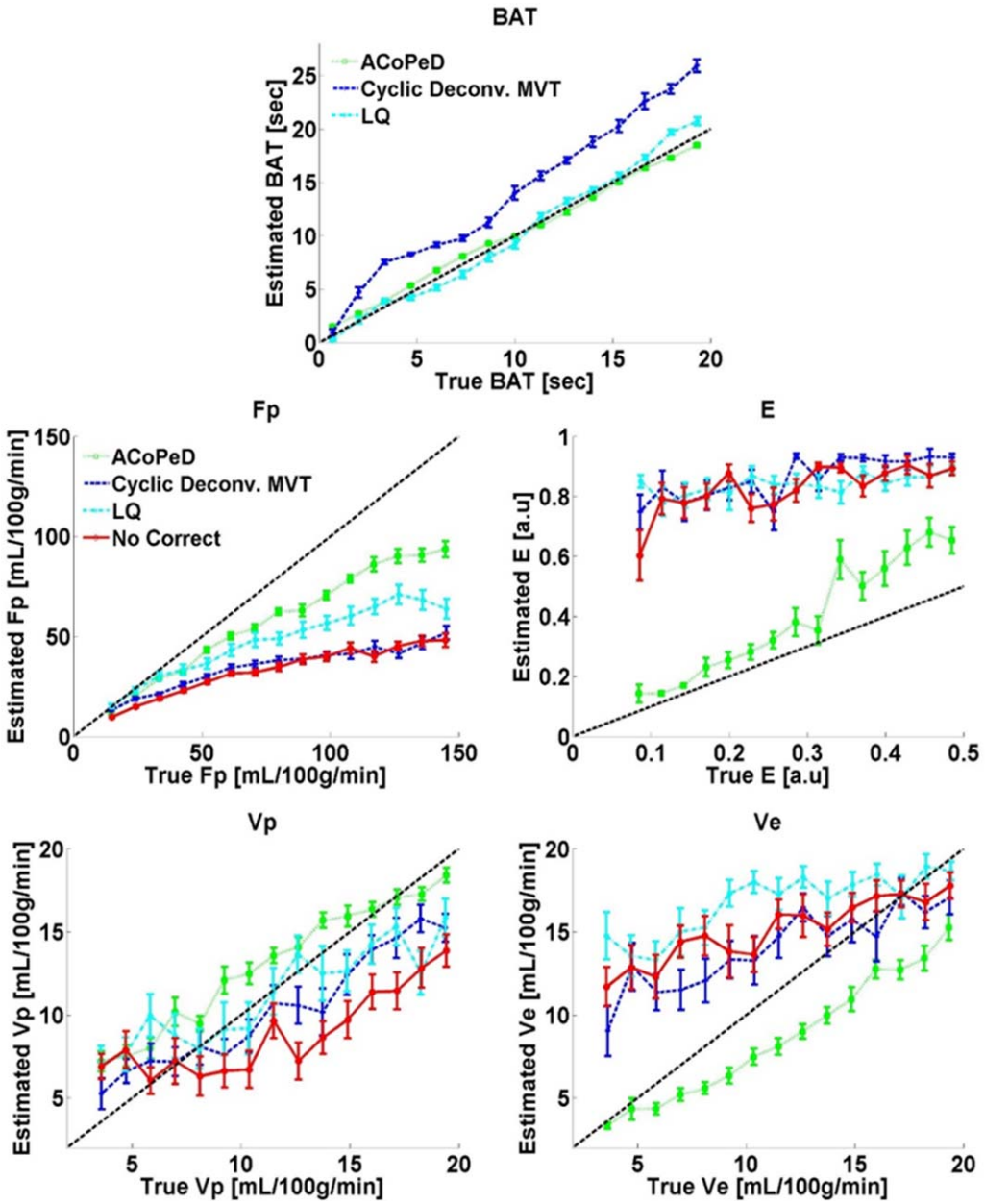

FIGURE 3: Estimating BAT and affected parameters. The different techniques: ACoPeD (green), circular deconvolution (blue), LQ-model (cyan), and no correction (red) was used for BAT correction and estimation. The top graph compares the different BAT estimation methods while the rest of the graphs show the effect of estimation on other PK parameters. Dashed black line = ground truth value.

DATA ANALYSIS. Preprocessing included brain extraction performed using the brain extraction module of the FSL toolbox (http://www.fmrib.ox.ac.uk/fsl),[24] and coregistration of all DCE volumes by rigid transformation using SPM8b realign module.[25] The DCE-MRI data was coregistered and converted to CTC in a standard fashion.[21] T_1 values were calculated with correction for inaccuracy of the flip angle as suggested by Liberman et al.[26] DCE-MRI data from patients was analyzed using ACoPeD with model selection. The AIF was defined to be the mean CTC from several voxels extracted manually from arteries in each patient. The same procedure was used to extract an average venous concentration–time curve in order to apply a partial volume effect correction method, as used by Sourbron et al.[4] In order to correct for partial volume effect, a mask was manually defined within the sagittal sinus, relative signal enhancement was calculated, and deconvolved with the AIF. The partial-volume correction factor is determined from the time-integral of the IRF. Conversion from blood volume and flow (v_b and F_b) to plasma (v_p and F_p) was done using an assumed hematocrit value of 0.45.[4] The displayed flow map was normalized by setting the mean F_p value in the normal-appearing white matter (NAWM) to 30 (mL/100g/min).[3,4] BAT estimation was performed with a temporal resolution of 0.1 seconds, and the range was set to be up to 5 seconds, a realistic value for high-grade glioma (indeed, no ceiling effect was evident in the results). Maps were filtered for signal intensity by removing voxels for which the median absolute CTC was less than 0.15% of the maximal median absolute signal in that scan.

TABLE 2. BAT Correction and Parameter Estimation

	Mean relative error ± SEM [%]			
	ACoPeD	**LQ**	**Cyclic deconv.**	**No correction**
F_P	24.32 ± 0.72	40.47 ± 1.01	48.81 ± 0.93	53.12 ± 0.74
E	55.14 ± 4.74	288.7 ± 12.8	277.6 ± 11.4	291.2 ± 13.1
v_p	33.97 ± 3.16	62.56 ± 3.32	46.64 ± 1.98	60.1 ± 2.42
v_e	31.91 ± 1.22	87.84 ± 4.85	74.26 ± 3.85	91.85 ± 4.88
BAT	22.13 ± 1.91	26.11 ± 2.15	59.90 ± 2.70	-

Mean relative error and standard error of the mean (SEM) [in %] of the bolus arrival time (BAT) and pharmacokinetic (PK) parameters, estimated using different methods for BAT correction.

DSC-MRI data analysis was performed using the PErfusioN Graphical User INterface (PENGUIN) software,[15] from which CBF and CBV maps were extracted (referred to as F-DSC). The estimation method in PENGUIN is according to Wu et al,[15] in which for every voxel the time signal curve is converted to CTC using the known relationship between T_2^* signal intensity and tracer tissue concentration. Maps of relative CBV are estimated by integrating the area under the CTC. Maps of relative CBF are estimated by measuring the height of each voxel's IRF. To obtain the IRF, an AIF, usually derived directly from imaging data, is deconvolved from the measured CTC using a block-circulant deconvolution matrix.

PK PARAMETER VALUES IN PATIENTS. PK values were extracted for the contralesional NAWM, normal-appearing gray matter (NAGM), and lesion in each patient. Semiautomatic threshold based segmentation of the lesion areas was performed using AnalyzeDirect software v. 11.0, (Mayo Clinic, Rochester, MN). Segmentation was performed on the postcontrast T_1-weighted images for the patients with GB and from fluid attenuation inversion recovery (FLAIR) images for the patients following stroke. The NAWM and NAGM masks were extracted from the precontrast T_1-weighted images using FMRIB's FAST algorithm (FAST, part of FSL). Mean values of F_p, v_p, v_e, E and BAT parameters were extracted from each mask.

COMPARISON BETWEEN DCE-MRI AND DSC-MRI. Comparison between DCE-MRI and DSC-MRI was conducted in one patient with GB and one patient following stroke, who had DSC-MRI data. For each subject, DCE-MRI v_p and F_p maps were realigned and resliced to the DSC-MRI space using SPM8b's rigid-body transformation module (MatLab statistical parametric mapping tool). Voxel-based correlations for blood flow and blood volume maps were performed where applicable according to the model selection maps

Statistical Analysis

SIMULATED DATA. For each parameter, the results obtained using different analysis methods were divided uniformly into 15 bins. In each bin, the mean relative error and the standard error of the mean (SEM) were calculated and compared. In addition, the mean relative error and the standard deviation (of the results compared to the simulated ground truth values), were calculated for F_p, v_p, v_e, E and BAT, extracted for each analysis method.

DATA FROM PATIENTS. Correlation between DCE-MRI and DSC-MRI for the flow and blood volume parameters was assessed using Pearson correlation coefficient. Significant correlations in this study were considered as $r \geq 0.25$ and $P < 0.05$.

Results

The optimized analysis method, ACoPeD, includes a 2nd derivative spline-based regularization term, BAT correction and model selection. The open-source MatLab implementation is available at: https://github.com/guyov1/DCE_perfusion. ACoPeD's total run time on 6 minutes of whole brain data with temporal resolution of 2 seconds was around 3 minutes on an Intel Xeon CPU with 16 cores @2.4 GHz when allowing parallelization on 10 cores. For every time shift, an additional overhead of 75% of the total run time was observed. For the given BAT search range of up to 20 seconds with 0.5 intervals, the total run time was 3+(20/0.5)*0.75*3 = 93 minutes.

Simulated Data

COMPARING DIFFERENT METHODS FOR PARAMETER ESTIMATION USING 2CXM. Table 1 summarizes the mean relative error in estimation of PK parameters over the entire parameter range, for the eight different estimation methods, seven with different deconvolution techniques and the direct four-parameter nonlinear fit. Figure 2 shows the estimation of each PK parameter versus its ground truth value for the best three deconvolution estimation techniques, in each category. The 2nd derivative regularized-spline technique resulted in the lowest mean error (F_p, v_p, v_e ~25%, E ~41%) while the direct four-parameter nonlinear fit

TABLE 3. Parameter Estimation: Choosing the Correct Model

	Mean error ± SEM [%]									
	Full model					Using the correct model				
	v_p	F_P	E	v_e	BAT	v_p	F_P	E	v_e	BAT
2CXM[1]+BAT[2]	26.41 ±1.54	21.72 ±13.09	19.98 ±17.12	27.29 ±0.94	8.70 ±4.50	26.41 ±1.54	21.72 ±13.09	19.98 ±17.12	27.29 ±0.94	8.70 ±4.50
2CXM	39.61 ±49.19	27.88 ±10.75	21.91 ±19.39	29.45 ±18.69	-	31.18 ±43.92	19.31 ±14.54	20.16 ±16.34	25.27 ±19.07	-
Uptake+BAT	85.72 ±95.97	51.75 ±13.69	54.13 ±44.04	-	13.03 ±10.43	34.71 ±23.25	52.61 ±10.69	56.82 ±50.21	-	12.37 ±8.72
Uptake	129.09 ±131.29	56.20 ±16.83	49.25 ±19.28	-	-	46.09 ±29.82	48.81 ±11.59	40.15 ±49.94	-	-
High. Vasc.[3]+ BAT	35.03 ±8.95	20.92 ±15.24	-	-	9.77 ±5.88	8.65 ±4.66	18.59 ±15.48	-	-	10.95 ±5.01
High. Vasc.	61.36 ±17.16	24.11 ±21.78	-	-	-	4.17 ±4.02	24.41 ±13.38	-	-	-
High. Perf.[4]+ BAT	46.67 ±9.78	-	-	-	11.30 ±7.30	1.63 ±1.21	-	-	-	12.60 ±6.85
High. Perf.	46.23 ±7.67	-	-	-	-	0.64 ±0.42	-	-	-	-

[1]2XCM – Two Compartment Exchange Model.
[2]BAT – Bolus Arrival Time.
[3]High. Vasc. – Highly Vascularized.
[4]High. Perf. – Highly Perfused.
Mean and standard error of the mean (SEM) [in %] of the 2CXM, compartment-uptake, highly vascularized, and highly perfused (with and without BAT) model parameters, estimated when assuming a full model of 2CXM+BAT and when using the correct ground truth model.

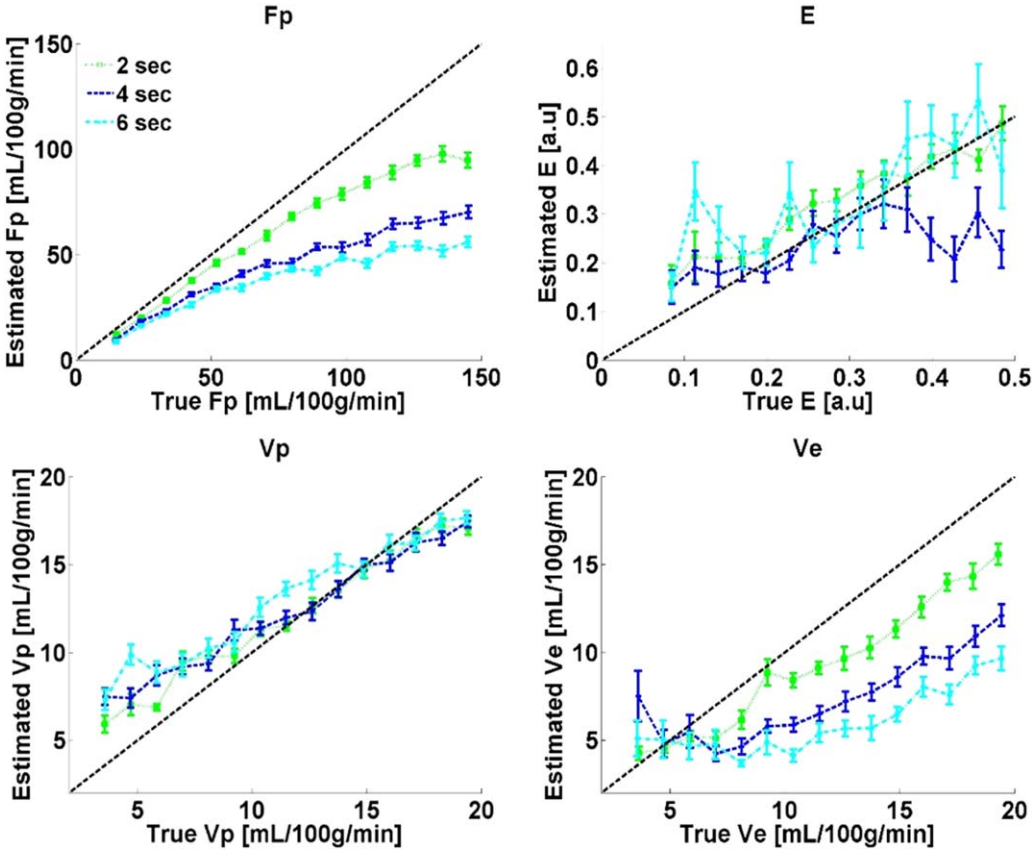

FIGURE 4: Estimation with different temporal resolutions. Using the spline with 2nd derivative method, the estimation process was repeated for varying temporal resolutions of 2 (green), 4 (blue), and 6 (cyan) second intervals. Degradation is apparent as resolution gets lower. v_p is more robust than the other parameters. Dashed black line = ground truth value.

resulted in the highest mean error (F_p, v_p, v_e ~80%, E ~190%). Thus, we used the 2nd derivative regularized-spline technique as the deconvolution method in ACoPeD, for the rest of the analyses.

BAT CORRECTION AND PARAMETER ESTIMATION. Figure 3 shows comparison of BAT and PK parameter estimation using three different methods for BAT estimation, and with no correction for BAT. ACoPeD, which includes the BAT correction procedure (described in Fig. 1), achieved the highest estimation accuracy for BAT parameters with mean error of 22.13 ± 1.91, compared to 26.11 ± 2.15 for the LQ-model and 59.90 ± 2.70 for the cyclic deconvolution MVT. All other PK parameters were also estimated with higher accuracy using ACoPeD compared to the other methods, with mean errors of: F_p: 24%, E: 55%, v_p: 34%, and v_e: 32%, over the entire range of PK values. Note that Fig. 3 shows the accuracy of estimation in one parameter, while the ground truth values of the other parameters are uniformly sampled from the range described above (simulated data). Relative errors over the entire range for the other BAT estimation methods are presented in Table 2.

CHOOSING THE CORRECT MODEL. Table 3 summarizes the result of parameter estimation when assuming a full model and when using the correct ground truth model. As seen, estimation accuracy is higher when using the correct ground truth model. As expected, the estimation accuracy improves when the ground truth model has fewer parameters.

EFFECT OF TEMPORAL RESOLUTION AND SCAN DURATION. Figure 4 shows the estimation error of the PK parameters as a function of the acquired temporal resolution. Mean relative errors over the entire range for all PK parameters are given in Table 4. As can be seen, the error in estimation of F_p, E, and v_e decreased when the temporal resolution was reduced from 6 to 2 seconds, and the differences are more pronounced at higher values. However, the v_p estimation seems to be less sensitive to the decrease in temporal resolution.

A longer scan duration, 20 minutes relative to 6 minutes, was shown to improve the estimation of all PK parameters. However, as expected, parameters that relate to the slow washout of contrast agent from extracellular space, ie, E and v_e are more sensitive to this factor (reduction in mean error: E: ~12%, v_e: ~6%).

Patient Data

PK PARAMETER VALUES IN PATIENTS. ACoPeD was used for estimation of parameters in seven patients: four

TABLE 4. Effect of Temporal Resolution and Scan Duration

	Mean relative error ± SEM [%]				
	Temporal resolution			Scan duration	
	2 sec	4 sec	6 sec	20 min	6 min
F_P	24.82 ± 0.67	39.18 ± 0.67	47.67 ± 0.68	21.84 ± 0.43	24.82 ± 0.67
E	41.72 ± 3.20	51.96 ± 3.5	84.66 ± 3.5	29.77 ± 3.11	41.72 ± 3.20
V_P	26.41 ± 1.54	29.18 ± 1.94	34.23 ± 2.30	23.53 ± 1.39	26.41 ± 1.54
V_e	27.29 ± 0.94	49.84 ± 2.74	56.90 ± 2.13	21.63 ± 0.95	27.29 ± 0.94
BAT[1]	-	-	-	-	-

Mean relative error and standard error of the mean (SEM) [in %] of the PK parameters, estimated using different acquisition parameters and scan duration.
[1]BAT – Bolus Arrival Time

patients with GB and three patients following stroke. Figure 5 shows a representative example of parameter maps obtained from a patient with GB (patient #4) using ACoPeD. In this case, only a negligible number of voxels resulted in a model that included BAT; therefore, only models without BAT are shown in Fig. 5F. The model selection map segmented the brain into GM (gray), WM (blue), and tumor (red and yellow).

Median values of the 2CXM parameters (after model selection process) for the NAGM, NAWM, and lesion for

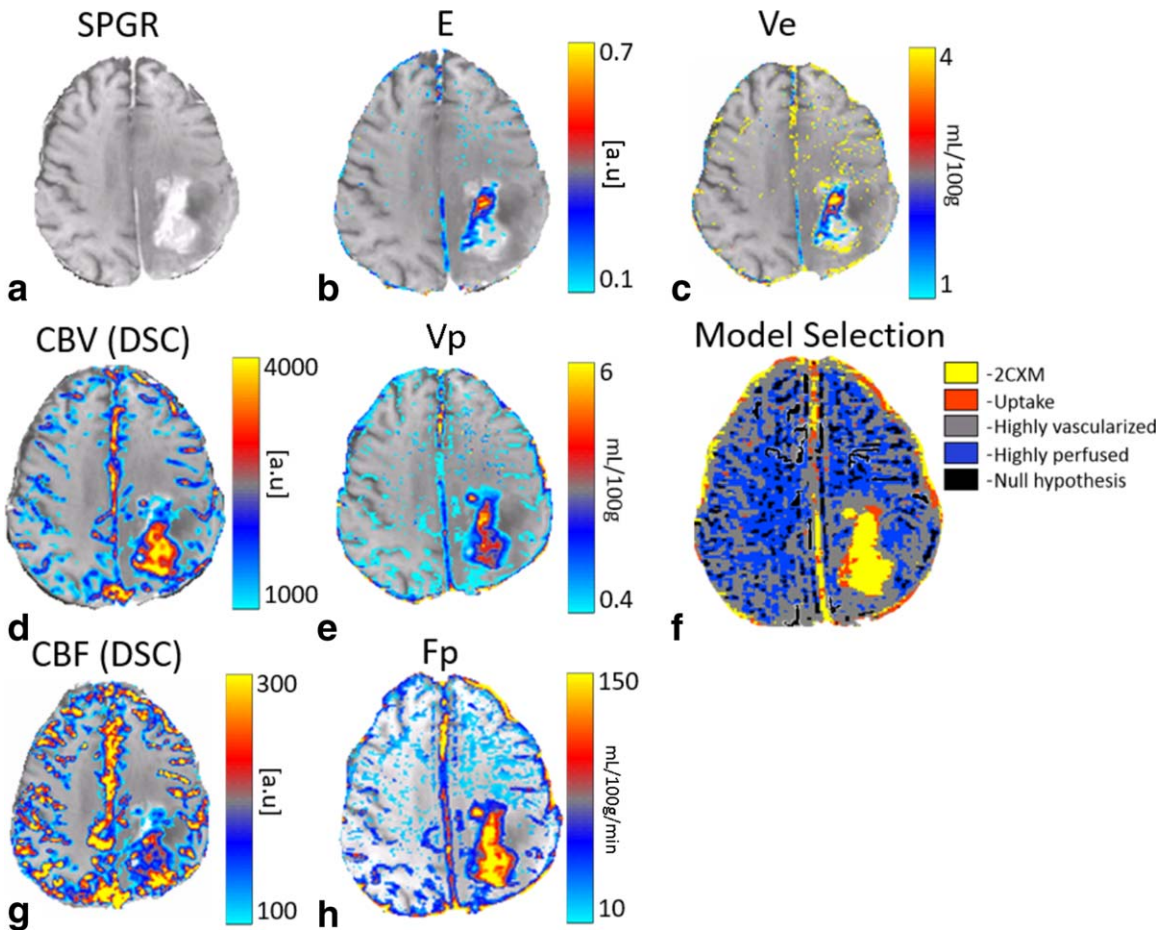

FIGURE 5: Parameters estimation in a high-grade tumor. DCE-MRI PK parameters extracted using ACoPeD, from a patient with brain tumor (B,C,E,H) on top of a postcontrast SPGR image (A). F: Model selection map. D,G: CBV and CBF maps extracted using DSC-MRI.

TABLE 5. Parameter Estimation in Patients

		Median value									
		F_p [mL/100g/min]			v_p [mL/100g]			v_e [mL/100g]		E [a.u.]	
	Patient	NAGM[1]	NAWM[2]	Lesion	NAGM	NAWM	Lesion	NAGM	NAWM	Lesion	NAGM	NAWM	Lesion
Stroke	1	38.42	26.48	34.30	1.20	0.85	1.20	NA	NA	NA	NA	NA	NA
	2	42.15	28.56	31.25	1.05	0.89	1.08	NA	NA	NA	NA	NA	NA
	3	44.42	24.73	26.00	1.50	0.80	1.22	NA	NA	NA	NA	NA	NA
GB	4	42.81	20.10	151.63	1.40	0.64	6.45	NA	NA	1.27	NA	NA	0.18
	5	39.28	28.89	58.83	1.10	0.89	6.57	NA	NA	6.59	NA	NA	0.17
	6	28.19	21.33	65.53	0.82	0.65	3.84	NA	NA	1.88	NA	NA	0.09
	7	24.81	24.06	31.51	0.94	0.87	2.72	NA	NA	5.77	NA	NA	0.10

Median of the 2CXM parameters estimated from patients, three following stroke and four with gliobastoma (GB).
[1]NAGM - contralesional hemisphere normal appearing grey matter
[2]NAWM - contralesional hemisphere normal appearing white matter

each patient are summarized in Table 5. As expected, both F_p and v_p are higher (1.5–2-fold) in the NAGM relative to the NAWM. The three patients with stroke, had no enhanced lesions, thus no v_e and E values were detected within the lesion. All three patients were scanned at the subacute phase (~5 days following the event) and showed some evidence for tissue reperfusion, thus the F_p and v_p within the lesion were similar to that of the NAWM. For the four patients with GB, all lesions were enhanced, and showed high F_p, v_p, v_e, and E values.

COMPARISON BETWEEN DSC-MRI AND DCE-MRI. Preliminary results in two patients (who had DSC-MRI data): one following stroke and the other with GB, demonstrated correlation between DCE-MRI and DSC-MRI. Figure 5 shows an example of parameter maps obtained from a patient with GB using ACoPeD, along with CBV and CBF maps obtained from DSC-MRI. Figure 6 shows parameter maps obtained from a patient following stroke; F_p and BAT maps estimated using ACoPed and CBF obtained from DSC-MRI, along with DWI image. High BAT values can be seen within the stroke lesion.

A significant ($P < 0.001$) voxel-based correlation was detected for blood flow between DCE-MRI and DSC-MRI in the patient following stroke ($r = 0.49$). In the patient with GB a weak correlation was detected ($P < 0.001$, $r = 0.2$). For blood volume, significant ($P < 0.001$) voxel-based correlations were detected between methods in the patient with GB ($r = 0.62$) and in the patient following stroke ($r = 0.35$).

Discussion

This study proposes ACoPeD: an optimized method for tissue perfusion and permeability estimation using DCE-MRI, based on 2CXM with spline-based deconvolution using 2nd derivative regularization, accounting for BAT, and incorporating model selection. The method was applied to simulated data, demonstrating the most accurate estimation of the PK parameters compared to other methods tested. Direct four-parameter estimation resulted in poorer estimation than the deconvolution based methods, which may stem from the complexity of the nonlinear four-parameter space. Incorporating the deconvolution technique results in a fair estimation of the plasma flow, and the direct three-parameter estimation of the resulting IRF seems to improve the estimation accuracy overall. High temporal resolution (2 sec) and long scan duration (20 min) were shown to provide more accurate results on simulated data. Simulation results showed that incorporating BAT and using the correct model significantly improved PK parameter estimation.

The choice of the most suitable model was suggested by Ewing et al[17] and Buckley and Sourbron[7] among others to have an important role in the interpretation of the

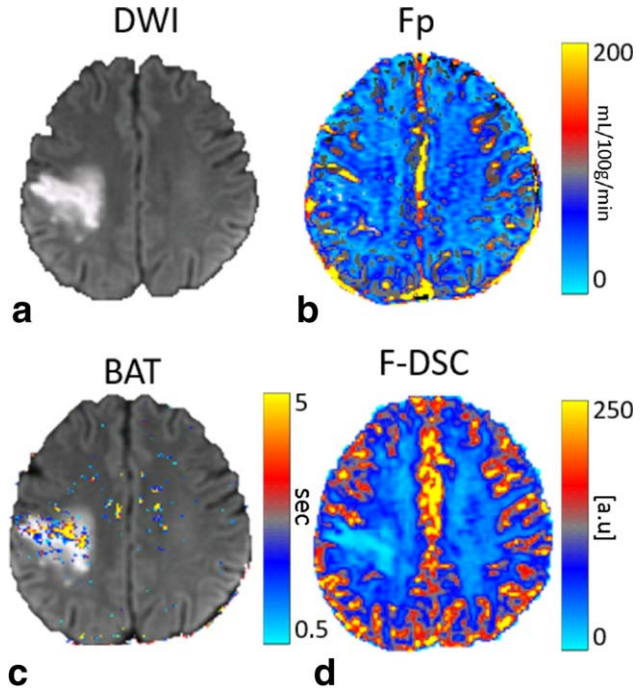

FIGURE 6: Parameter estimation in stroke. DCE-MRI Fp and BAT maps (B,C) extracted by the ACoPeD tool from a patient following stroke on top of a diffusion-weighted image (A). D: CBF map extracted using DSC-MRI.

extracted PK maps. Results from this study are in line with their findings. In this study, models with and without BAT were selected according to the corrected Akaike information criterion. BAT was shown to improve the estimation of the PK parameters in simulated data. The method was applied to data of patients with brain tumors and patients following stroke. The model selection map segmented the brain tissue in patients with brain tumor into GM, WM, and tumor area, reflecting the different vascular properties of the normal and pathological brain tissue components, and may have a clinical role in patient assessment and follow-up.

Incorporating flow in DCE-MRI analysis has been previously proposed,[2–4,11] yet the applicability of such a method in clinical settings is still limited. Currently, DSC-MRI is the method of choice to detect cerebral blood flow in patients following stroke and patients with brain tumors. However, there are several inherent drawbacks to the DSC-MRI method including the relatively low spatial resolution and high sensitivity to susceptibility artifacts, such as in regions containing blood, calcification, metallic surgical materials, and in areas adjacent to the temporal lobes or skull base. In stroke patients, DSC-MRI provides the required clinical information regarding the location and amount of reduced perfusion with high sensitivity, and has higher CNR in areas of WM relative to DCE-MRI. In addition, susceptibility artifacts are less common in patients following stroke, and during the acute phase the lesion permeability is intact. Therefore, DSC-MRI seems to be preferable in the case of a stroke over DCE-MRI. On the contrary, in patients with brain tumors the information regarding permeability is of great clinical importance, high spatial resolution images are preferable due to the highly heterogeneous nature of high-grade tumors, and susceptibility artifacts are more common. Using the 2CMX model enables acquisition of all vascular parameters in one method, which requires only a single dose of contrast agent. Thus, in patients with brain tumors, DCE-MRI using the 2CMX model might be preferable over DSC-MRI. While this study focused on cerebral perfusion, the quantification methods may equally be applicable to other organs.

Several limitations to this study should be addressed regarding technical and study design: Accurate estimation of PK parameters was shown to require high temporal resolution. Acquiring high temporal and spatial resolution data currently results in reduced brain coverage. Therefore, our results are based on only a few slices. However, with new MRI technologies that enable increased brain coverage with high temporal resolution, this method may be routinely used for patient assessment and diagnosis. In the conversion of signal to concentration, the precise influence of limited water exchange[27] was ignored. In addition, the postprocessing time was relatively long. However, since the voxelwise calculations are independent it can be easily parallelizable for multicore processors or graphical processing units. With regard to study design, this study shows results on a relatively small number of patients and the comparison to DSC-MRI was performed in only two patients. Additional studies are needed to confirm and validate our results and evaluate the contribution of this method in other neurological disorders.

In conclusion, this study proposes the ACoPeD tool—a robust approach for flow estimation using DCE-MRI data in clinical setup. An open source implementation is publicly available, aiming to improve standardization of DCE-MRI and to enable the analysis of routinely acquired clinical data with the 2CXM model.

Acknowledgments

Contract grant sponsor: Yitzhak and Chaya Weinstein Research Institute for Signal Processing

We thank Vicky Myers for editorial assistance. This work was performed in partial fulfillment of the requirements for an MSc degree of Guy Nadav, School of Electrical Engineering, Tel Aviv University, Israel.

References

1. Sourbron SP, Buckley DL. Classic models for dynamic contrast-enhanced MRI. NMR Biomed 2013;26:1004–1027.

2. Larsson HB, Hansen AE, Berg HK, Rostrup E, Haraldseth O. Dynamic contrast-enhanced quantitative perfusion measurement of the brain using T1-weighted MRI at 3T. J Magn Reson Imaging 2008;27:754–762.
3. Larsson HB, Courivaud F, Rostrup E, Hansen AE. Measurement of brain perfusion, blood volume, and blood-brain barrier permeability, using dynamic contrast-enhanced T1-weighted MRI at 3 tesla. Magn Reson Med 2009;62:1270–1281.
4. Sourbron S, Ingrisch M, Siefert A, Reiser M, Herrmann K. Quantification of cerebral blood flow, cerebral blood volume, and blood-brain-barrier leakage with DCE-MRI. Magn Reson Med 2009;62:205–217.
5. Fluckiger JU, Schabel MC, DiBella EV. Toward local arterial input functions in dynamic contrast-enhanced MRI. J Magn Reson Imaging 2010;32:924–934.
6. Liberman G, Louzoun Y, Colliot O, Ben Bashat D. T1 Mapping, AIF and pharmacokinetic parameter extraction from dynamic contrast enhancement MRI data. Multimodal Brain Image Anal 2011;7012:76–83.
7. Sourbron SP, Buckley DL. On the scope and interpretation of the Tofts models for DCE-MRI. Magn Reson Med 2011;66:735–745.
8. Ingrisch M, Sourbron S, Morhard D, et al. Quantification of perfusion and permeability in multiple sclerosis: dynamic contrast-enhanced MRI in 3D at 3T. Invest Radiol 2012;47:252–258.
9. Ahearn T, Staff R, Redpath T, Semple S. The use of the Levenberg-Marquardt curve-fitting algorithm in pharmacokinetic modelling of DCE-MRI data. Phys Med Biol 2005;50:N85–92.
10. Irving B, Tanner L, Enescu M, et al. Personalised estimation of the arterial input function for improved pharmacokinetic modelling of colorectal cancer using dceMRI. In: Abdominal imaging computation and clinical applications. New York: Springer; 2013. p 126–135.
11. Kershaw LE, Buckley DL. Precision in measurements of perfusion and microvascular permeability with T1-weighted dynamic contrast-enhanced MRI. Magn Reson Med 2006;56:986–992.
12. Calamante F, Willats L, Gadian DG, Connelly A. Bolus delay and dispersion in perfusion MRI: implications for tissue predictor models in stroke. Magn Reson Med 2006;55:1180–1185.
13. Østergaard L, Weisskoff RM, Chesler DA, Gyldensted C, Rosen BR. High resolution measurement of cerebral blood flow using intravascular tracer bolus passages. Part I: Mathematical approach and statistical analysis. Magn Reson Med 1996;36:715–725.
14. Calamante F, Gadian DG, Connelly A. Delay and dispersion effects in dynamic susceptibility contrast MRI: simulations using singular value decomposition. Magn Reson Med 2000;44:466–473.
15. Wu O, Østergaard L, Weisskoff RM, Benner T, Rosen BR, Sorensen AG. Tracer arrival timing-insensitive technique for estimating flow in MR perfusion-weighted imaging using singular value decomposition with a block-circulant deconvolution matrix. Magn Reson Med 2003; 50:164–174.
16. Liberman G, Louzoun Y, Artzi M, Nadav G, Ewing JR, Bashat DB. DUSTER: Dynamic contrast enhance up-sampled temporal resolution analysis method. Magn Reson Imaging 2016;34: 442–450.
17. Cheong L, Koh T, Hou Z. An automatic approach for estimating bolus arrival time in dynamic contrast MRI using piecewise continuous regression models. Phys Med Biol 2003;48:N83–88.
18. Bagher-Ebadian H, Jain R, Nejad-Davarani SP, et al. Model selection for DCE-T1 studies in glioblastoma. Magn Reson Med 2012;68: 241–251.
19. Parker GJ, Roberts C, Macdonald A, et al. Experimentally-derived functional form for population-averaged high-temporal-resolution arterial input function for dynamic contrast-enhanced MRI. Magn Reson Med 2006;56:993–1000.
20. Bishop CM. Pattern recognition and machine learning. New York: Springer; 2006.
21. Gobbel G, Fike J. A deconvolution method for evaluating indicator-dilution curves. Phys Med Biol 1994;39:1833–1854.
22. Liberman G, Nadav G, Louzoun Y, Artzi M, Ben Bashat D. Bolus arrival time extraction using super temporal resolution analysis of DCE. In: Proc 22nd Annual Meeting ISMRM, Milan; 2014.
23. Essig M, Nguyen TB, Shiroishi MS, et al. Perfusion MRI: the five most frequently asked clinical questions. AJR Am J Roentgenol 2013;201: W495–510.
24. Smith SM. Fast robust automated brain extraction. Hum Brain Mapp 2002;17:143–155.
25. Wells WMI, Viola P, Atsumi H, Nakajima S, Kikinis R. Multi-modal volume registration by maximization of mutual information. Med Imag Anal 1996;1:35–51.
26. Liberman G, Louzoun Y, Ben Bashat D. T1 Mapping using variable flip angle SPGR data with flip angle correction. J Magn Reson Imaging 2014;40:171–180.
27. Buckley DL, Kershaw LE, Stanisz GJ. Cellular-interstitial water exchange and its effect on the determination of contrast agent concentration in vivo: Dynamic contrast-enhanced MRI of human internal obturator muscle. Magn Reson Med 2008;60:1011–1019.